Propeller selection based on real weather conditions

Maxime Steelandt
Instituto Superior Técnico, Universidade de Lisboa, Portugal

Abstract- **This article presents an alternative method to select the best Wageningen B-series propeller for a ship. The alternative method selects the propeller based on a given sea state. This alternative method is based on simulations of the ship and propeller in a given sea state and selects the propeller with the highest delivered efficiency for that given sea state. In the simulations, propeller ventilation, varying added resistance and varying advance speed are taken into account. The last two factors are calculated by the 'quasi' regular wave approach that was proposed in [1]. The alternative method is applied to the KVLCC2 tanker and S175 container ship and compared to the commonly used selection procedure for the ships in still water. The differences between the propellers selected by the different methods were small and the increase of performance negligible. However, the differences could be explained by the increase of the average advance speed and the added resistance. Furthermore it was concluded that to reduce cavitation the average added resistance could be taken into account for the propeller selection in still water.**

Keywords- **Wageningen B-series, propeller selection, propulsion in waves, irregular waves**

I. Introduction

The world today is using more resources than it can produce in a year. Because of our growing conscience that this is not sustainable, the call for energy efficient devices is high and the world's leading research institutes are focusing on increasing efficiency in all of their facets. It is very important to utilise the energy resources with utmost care or the future world will end up with a deficiency of them. Furthermore the use of fossil fuels causes a lot of pollution, especially in ships, where more polluted fuels and less filters are used. The maritime industry, as one of the biggest consumers of fossil fuels, has been alerted to this fact. In 2018, the IMO (International Maritime Organisation) made a long term strategy to reduce the annual amount of green house gas emissions by 50% by 2050[2]. So, the study of energy efficient ships and the factors affecting them is of paramount importance.

The choice of propeller is key in order to have a ship with good efficiency. In modern shipbuilding the propeller is optimised as if the ship is sailing in still water, although most ships will barely sail in still water. The effect of waves on the propeller are yet to be clearly understood. It has been observed that the propeller reacts to the time varying flow field encountered in waves, and it would be useful to consider the effect of waves on the propeller already in the design stage. In case of propeller emergence, when the propeller is coming partly out of the water, the propeller thrust and torque drop significantly. Furthermore, the resistance of the ship varies when the ship is encountering waves. Some research has already been conducted regarding those influences and some models were proposed. Yet, these models have not been implemented in the selection procedure of a propeller. Using this knowledge in the selection of propellers in waves could help to reach the goals set by the IMO.

Therefore, an alternative propeller selection procedure for single open propellers with constant pitch is developed and discussed. The selection is carried out for the Wageningen B-series propellers the help of the built-in Matlab function *'fmincon'* which optimises the delivered efficiency in waves. The delivered efficiency in waves is calculated by a custom built Matlab function. This function simulates the ship and propeller sailing in waves in time and space domain and takes into account several effects of waves on the propulsion. An overview of the effects of waves on the performance is shown in fig. 1. The effects shown in grey are not modelled in the proposed selection method due to their complexity and sometimes limited influence. The varying wake and added resistance are calculated by the 'quasi' regular wave approach as proposed in [1]. Inspiration of the time domain simulation is taken from [3], which is also the main reference used to validate the simulation code.

The selection, and thus also the simulation, is made in such way that it can run for regular or irregular waves. Furthermore, the simulation also works for a sequence of different wave profiles to allow the selection based on a scatter diagram. In order to run the selection code the ships characteristics are required. These are calculated by a code developed at CENTEC which has been used previously used in [4] and [5]. This code computes three types of characteristics:

- **Still water resistance** according to [6]
- **Ship motions in the frequency domain** according to the strip theory as formulated in [7].
- **Added resistance in head and bow waves** according to the far-field theory as formulated in [8].

This alternative selection procedure is used to select the optimal propeller for the KVLCC2 tanker and the S175 containership for different sea states. These propellers are compared to the optimal in still water. The aim of this alternative selection procedure is to increase the real life efficiency of the ship.

II. Simulation model

The simulation model used was mainly verified by comparing the obtained results with the results in [3], however the

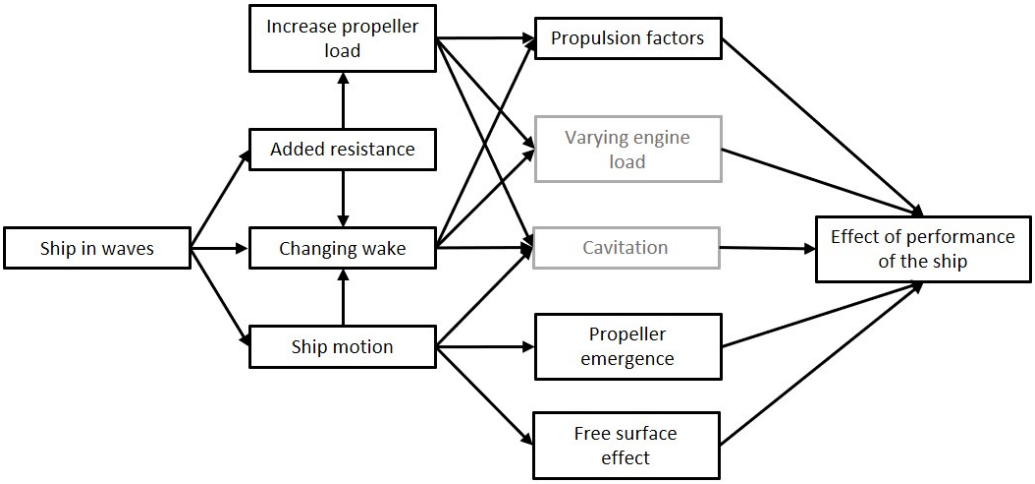

Fig. 1: The effects of waves on ship propulsion

simulation model is not the same. In the reference paper the shaft and engine are modelled while these are not included in this simulation model. Instead, the propeller was given a constant rotational speed that is required to propel the ship at service speed in still water. This rotational speed and the time dependent wake velocity are used as inputs for the propeller model, which computes the thrust and torque. The thrust is used by the vessel model to update the ship's speed based on the ship's resistance and inertia. The torque is used for the calculation of the delivered efficiency. The verification of the simulation results are done for the KVLCC2 whose main characteristics are given in table I.

L_{PP} $[m]$	320
L_{WL} $[m]$	325.5
B $[m]$	58
d $[m]$	20.8
Δ $[ton]$	312622
C_B	0.8098
U_S $[kn]$	15.5
x_P $[m]$	$-0.49L_{PP}$
z_P $[m]$	$-0.045L_{PP}$

TABLE I: Ship particulars of the KVLCC2

Additionally several RAO's are compared to the ones given in [3]. The pitch RAO is required to calculate mean increase in propeller inflow using the method decribed in [1] which is discussed later in section II-C. The RAO for relative stern motion has been used to compute variation in thrust and torque due to the variation in propeller submergence in different wave conditions. These RAO's can be seen in figs. 2-4. The phase of the relative motion RAO does not match with the one given in [3]. This is explained by the fact that in the seakeeping code, developed at CENTEC, the regular waves are assumed to have a through on the position of the centre of gravity. This results in phase of the motions to have a 180° shift with respect to the usual convention. Furthermore, the surge motion RAO is necessary to compute wake fluctuations in waves using the model described in [9] which is discussed later in section II-C. However, the surge motion could not be calculated by the linear strip theory method that is implemented in the seakeeping code developed at CENTEC. Therefore, the RAO of surge is based on the graph given in [3].

A. Resistance model

The total resistance is computed by adding the still water resistance and the added resistance together. The still water resistance for the given speed is found by interpolation of the still water resistances calculated by code developed at CENTEC. The added resistance is assumed to be constant for regular waves and is calculated using formula 1. The added resistance in irregular waves is calculated by the 'quasi' regular wave approach as proposed in [1] and used in [10]. This approach converts an irregular sea state into a train of regular waves by locating the zero up-crossing (zero down-crossing) points. The period of the 'quasi' regular wave is equal to the time between the previous and the upcoming zero up-crossing and the wave amplitude is equal to the average of the lowest trough and the highest crest withing that period. Both parameters change in an irregular sea so the 'quasi' regular wave changes as well during the simulation. Based on the 'quasi' regular wave properties of the wave at midships, the added resistance is then computed using formula 1. This method was adopted to make the added resistance vary between different waves.

$$\overline{R_{add}}(U) = A_w^2 \Phi_{AW}(\omega, U) \tag{1}$$

Where Φ_{AW} is the dimensional added resistance coefficient is calculated as follows:

$$\Phi_{AW} = \sigma_{AW}(\omega)\rho g B^2 L_{PP}^{-1} \tag{2}$$

σ_{AW} is the added resistance coefficient calculated using code developed at CENTEC.

B. Ventilation model

In order to consider the effect of waves on the propulsion of the ship, thrust and torque losses due to propeller emergence, free surface effect and Wagner effect have been modelled. Thrust loss in case of propeller emergence has been assumed

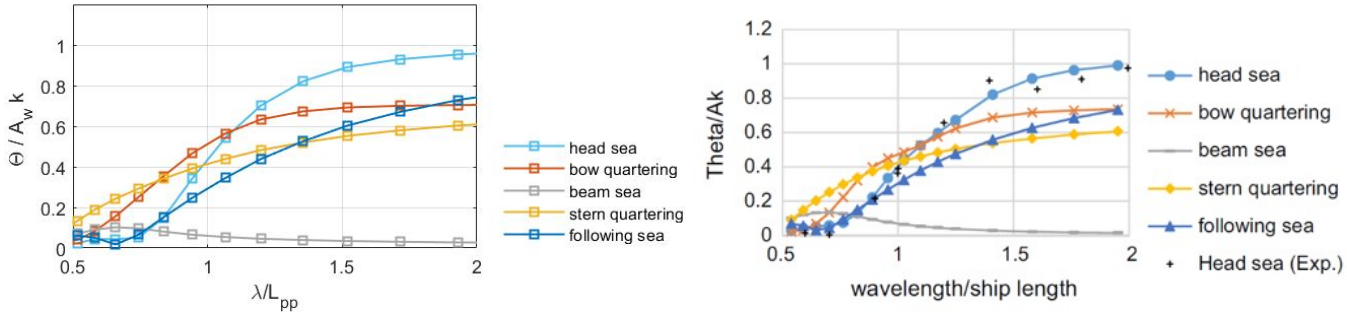

Fig. 2: Comparison of the RAO of pitch amplitude used in the simulation (left) and used in [3](right)

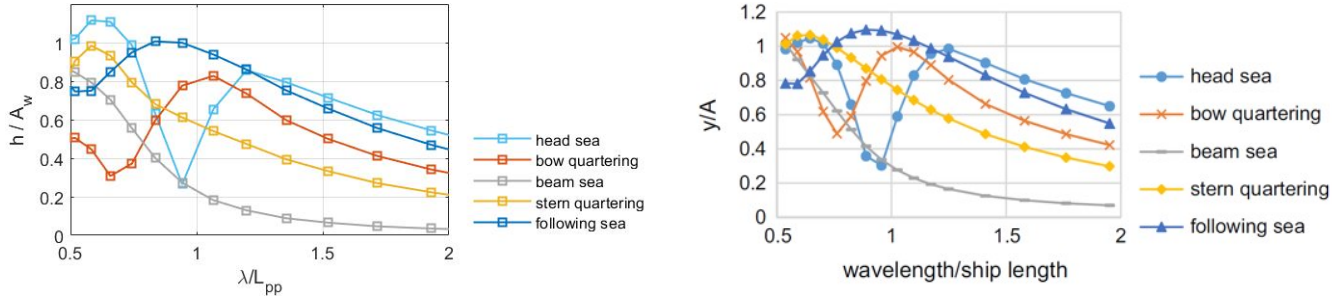

Fig. 3: Comparison of the RAO of relative motion amplitude used in the simulation (left) and used in [3](right)

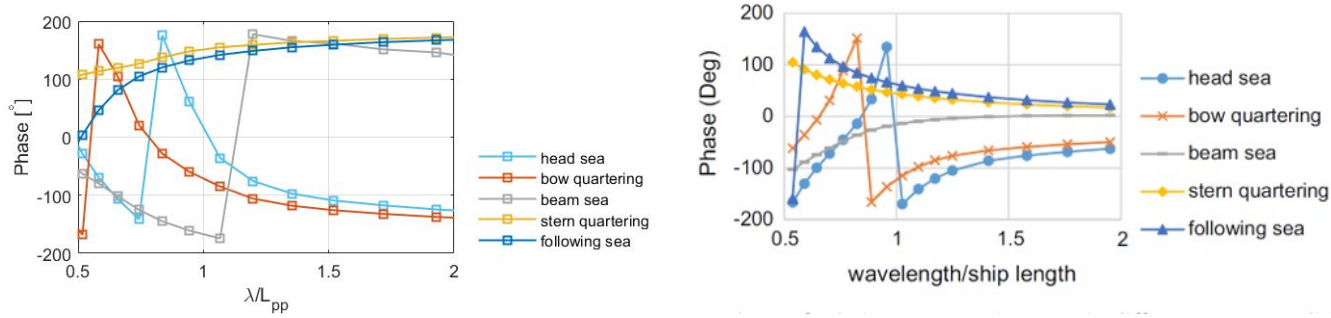

Fig. 4: Comparison of the RAO of relative motion phase angle used in the simulation (left) and used in [3](right)

proportional to the out of water area of the propeller disc as suggested in [1]. In case of propeller emergence, propeller blades take some time to develop the lift once they re-enter the water and thereby reducing average thrust and torque. This effect has been considered in terms of average thrust and torque loss as suggested in [11]. In addition, thrust and torque is lost when the propeller operates close to the free surface generating waves on the free surface due to propeller action. These effects have been included by using thrust loss factor given in equation as proposed in [11]. This model is said to be convenient when only the averages are of interest [12] and therefore is used in the simulation.

$$\beta_T = \begin{cases} 0 & \frac{h}{R} \leq -0.48 \\ 1 - 0.675(1 - 0.769\frac{h}{R})^{1.258} & -0.48 \leq \frac{h}{R} \leq 1.3 \\ 1 & 1.3 \leq \frac{h}{R} \end{cases} \quad (3)$$

This loss factor is not the same for the torque, the torque loss factor is computed as follows:

$$\beta_Q = \beta_T^m \quad (4)$$

The factor m takes into account that there is less torque loss than thrust loss. This was noticed in [1], m is set at 0.83 because this is in the median of the range given in that paper.

C. Wake velocity model

The advance speed is modelled according to equation 5. In this calculation the 'quasi' regular wave approach has been applied because superposition of different waves frequencies is not valid due to the non-linearities in the model (e.g. the α-factor and exponential with wave number). The model requires the wake factor (w_s) in still water which is calculated according to [13] for the S175. For the KVLCC2 this method gave a values of around 0.1 lower than in measurements given in

[14], therefore it is forced to the value of the measurements in order to allow a fair comparison.

$$U_{A,total} = U_{A,fluctuating}\frac{U_{A,mean}}{U} \tag{5}$$

Where $U_{A,fluctuating}$ is the fluctuating part of the advance speed calculated by equation 6 as proposed in [9]. $U_{A,mean}$ is the mean increase of propeller inflow velocity calculated by equation 8 as proposed in [1].

$$\begin{aligned} U_{A,fluctuating} =&(1-w_s)(U-\omega_e|z_1|\sin(\omega_e t-\zeta_1)) \\ &+\alpha\omega A_w \exp(-kz_P)\cos\chi \\ &\cos(\omega_e t - kx_P\cos\chi) \end{aligned} \tag{6}$$

Where $|z_1|$ is the surge amplitude, ζ_1 the surge phase and α is a coefficient representing the effect of wave amplitude decrease at the stern given as follows:

$$\alpha = \begin{cases} 0.2\frac{\lambda}{L_{PP}|\cos\chi|}+0.5 & \frac{\lambda}{L_{PP}|\cos\chi|}\leq 2.5 \\ 1 & \frac{\lambda}{L_{PP}|\cos X\chi|}>2.5 \end{cases} \tag{7}$$

$$U_{A,mean} = U\sqrt{1-\frac{\Delta\bar{p}}{0.5\rho U^2}} \tag{8}$$

Where $\Delta\bar{p}$ is the mean pressure increase due to pitching of the ship, this is estimated by equation 9 as proposed in [1].

$$\Delta\bar{p} \sim -\frac{\rho}{4}\omega_e^2|z_5|^2x_P^2 \tag{9}$$

Where $|z_5|$ is the pitch amplitude.

The model of the mean increase (eq. 8) for the KVLCC2 is compared to measurements found in [14] and also by simulations done in [3], this is summarised in table II. Furthermore, the wake velocities including as calculated by equation 5 are also compared to those two references as shown in fig. 5. These comparisons are made for the ship sailing at constant design speed, not taking into account the balance between propeller thrust and ship resistance, thus the wake varies only due to the ship motions.

λ/L_{PP}	A_w	% increase in mean wake velocities		
		Model	Simulations in [3]	Experiments [14]
0.6	3	0.00%	0.03%	0%
1.1	3	2.50%	2.70%	5.0%
1.6	3	2.14%	2.66%	2.2%

TABLE II: Comparison of increase in mean propeller inflow due to pitch in head waves using formula and experiments

D. Propeller model

In the selection propeller procedure the best Wageningen B-series propeller is selected, the characteristics of the B-series are modelled by the Oosterveld polynomials [15]. The theoretical torque and thrust are calculated by the K_Q and K_T polynomials. The effective torque and thrust are then found by multiplying the theoretical values with β_Q and $(1-t_s)\beta_T$. The still water thrust reduction factor (t_s) and is computed by the code developed at CENTEC according to the method described in [6]. In [16] is was noticed that the thrust deduction factor varies in presence of waves. Nevertheless, the still water thrust reduction factor is used because the effect of the variations is negligible in most cases [17].

In [3] similar simulations as for the wake were done for the torque but with an increased wave amplitude of 5 meters. In those simulations, the varying wake factor and ventilation were included and the ship was sailing at a constant speed of 14.7 knots. The propeller used in the simulation was the $B4-43.2$ with $P/D = 0.47$ and $D = 9.86$ but with a skew of 21.15° instead of 0° in the normal B-series. The skew does not have a significant effect on the torque and could not me modelled in the used propeller model. Therefore, simulations made by the model with normal B-series propeller are compared to the simulations given in [3]. The comparison is shown in figs. 6-8. The torque amplitudes are not matching the reference exactly but they are with acceptable limits. The average of the torque is higher than in the simulations of the reference this might be partly explained by the skew. In fig. 8 the effect of the ventilation can be seen in the reference simulation while this is not present in the simulation. This could not be explained until now and an email was send to the author of the reference who on the moment of writing could not explain why there is ventilation in fig. 8 and not in fig. 7 while the RAO of the relative motion is the more or less the same for both wavelengths.

E. Vessel model

A simple vessel model (eq. 10) based on Newton's first law has been implemented to include vessel dynamics in the simulations.

$$M\frac{\mathrm{d}U}{\mathrm{d}t} = T_{eff} - R_T \tag{10}$$

Where M is the sum of the mass of the ship (m) and the hydrodynamic added mass of surge (m_{11}). This added mass cannot be calculated by the 2-D strip theory that is used in the code developed at CENTEC, therefore the following empirical formula suggested in [18] is used:

$$m_{11} = \frac{m}{\pi\sqrt{\rho L_{pp}^3/m}-14} \tag{11}$$

III. Proposed selection model

As mentioned earlier the proposed propeller selection procedure based on the ship in waves, selects the propeller with the highest delivered efficiency in the given sea state. This is efficiency is calculated using the following equation:

$$\eta_D = \overline{\left(\frac{P_E}{P_D}\right)} = \overline{\left(\frac{R_T U}{NQ_{eff}}\right)} \tag{12}$$

As the propellers considered are the Wageningen B-series, the propeller is defined by four parameters that define the propeller: the number of blades, pitch ratio, expanded blade ratio and the diameter of which the number of blades is fixed in the selection procedure. The other parameters are limited by eleven boundary conditions:

- **Six linear inequalities**, namely each parameter is limited by an upper and a lower value based on the original B-series measurements.

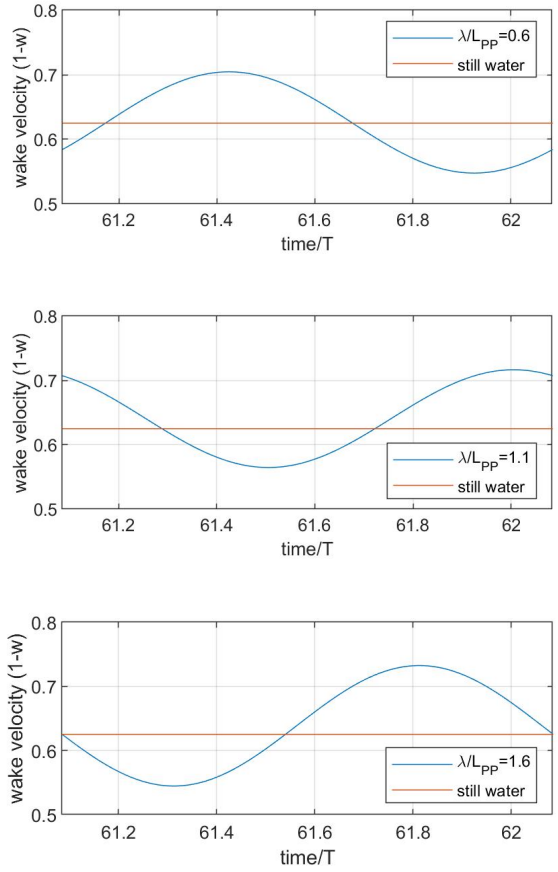

(a) Simulation

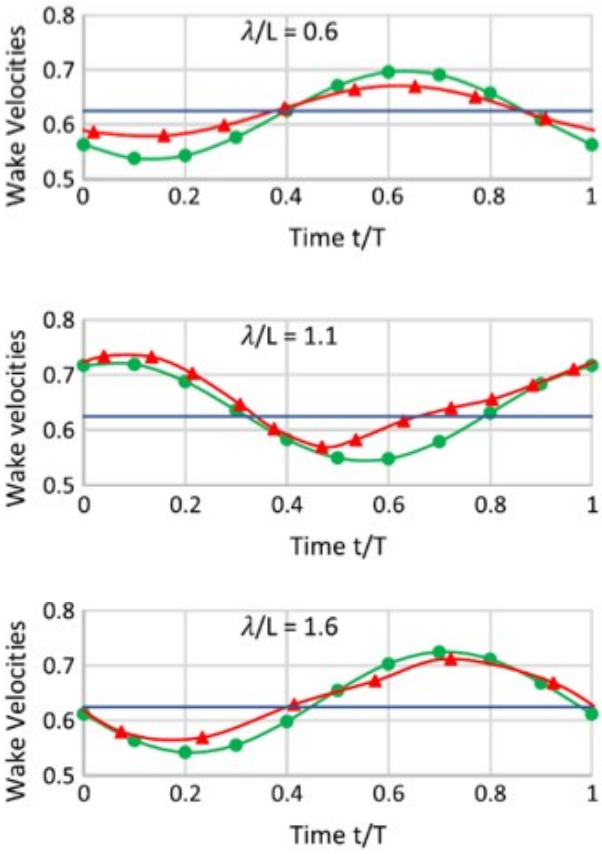

(b) Green: simulations of [3] Red: measurements [14], Blue: still water

Fig. 5: Simulations of the fluctuating wake

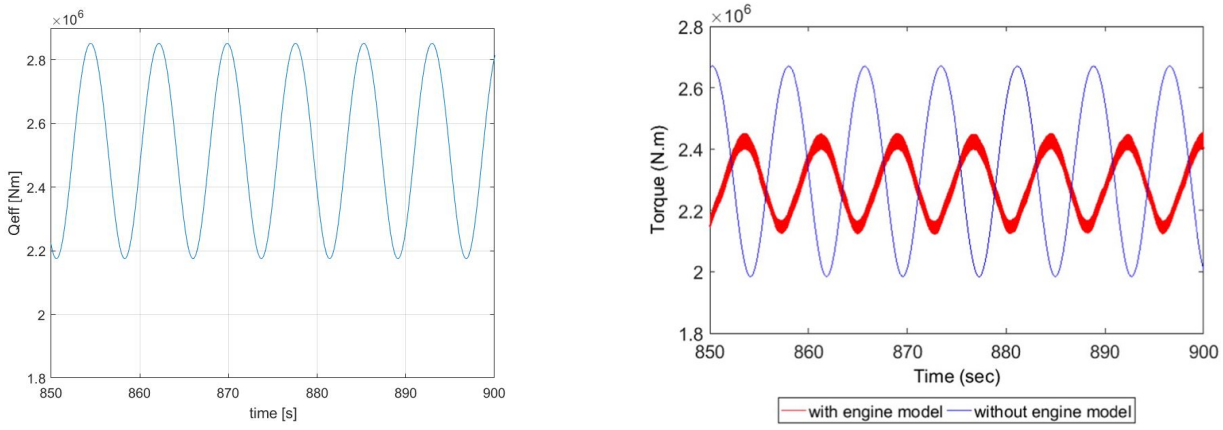

Fig. 6: Comparison of the torque by the simulation code (left) and torque of the reference simulation (right) [3] for $\lambda/L_{PP} = 0.6$

- **Five non-linear inequalities** of which two inequalities verify if the propeller can deliver the required thrust to maintain the service speed in still water within the limits of the engine speed (lower and upper limit). Two other inequalities verify if the delivered power for the ship in still water at service speed is within defined power limits. The fifth non-linear inequality verifies if the 5% cavitation criteria of Burrill [19] is satisfied for the propeller working in still water and the ship at service speed.

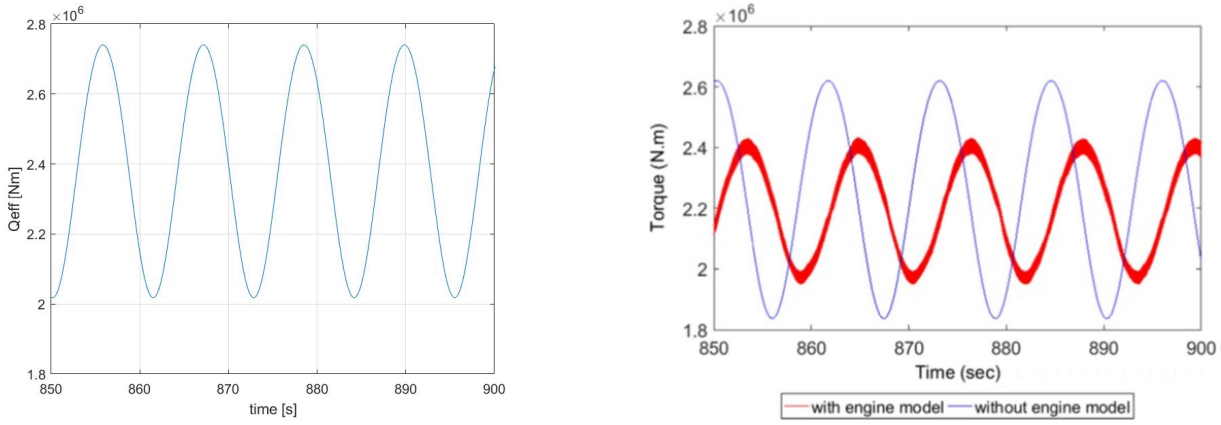

Fig. 7: Comparison of the torque by the simulation code (left) and torque of the reference simulation (right) [3] for $\lambda/L_{PP} = 1.1$

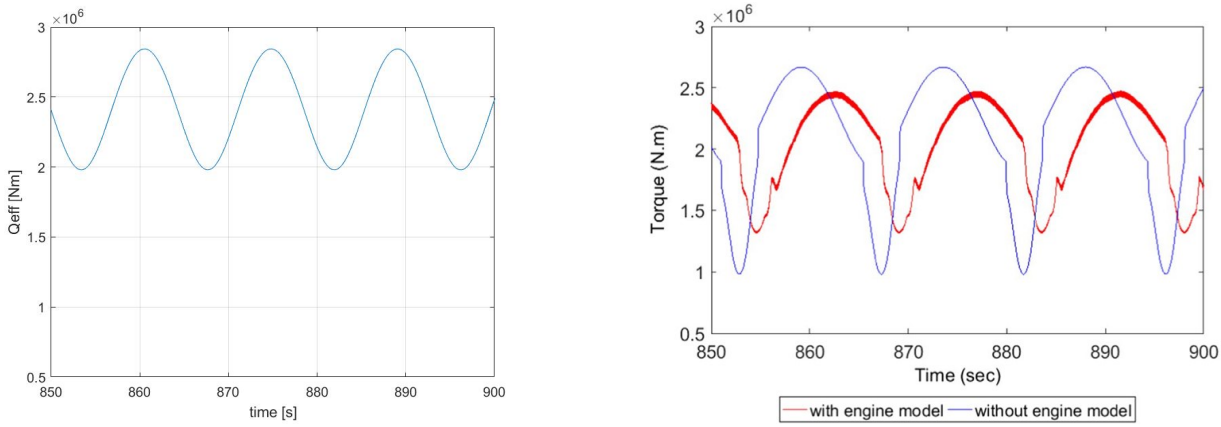

Fig. 8: Comparison of the torque by the simulation code (left) and torque of the reference simulation (right) [3] for $\lambda/L_{PP} = 1.6$

IV. Discussion of the results

The propeller selection procedure is applied to select propellers for the KVLCC2 tanker and the S175 containership in head waves for four different conditions: one still water condition and three different sea states based on the DNV North Atlantic scatter diagram. These three sea state are:

- **SS1**: the most probable sea state ($H_s = 1.5m$ and $T_p = 7.5s$)
- **SS2**: the average sea state ($H_s = 3.4m$ and $T_p = 8.9s$)
- **SS3**: a rough sea state based with a probability of 2.4%. ($H_s = 5.5m$ and $T_p = 9.5s$)

Additionally, a propeller is also selected based on a scatter diagram for the S175. This scatter diagram is a reduced version of the DnV North Atlantic scatter diagram, only the sea states with a probability of occurrence higher than 5% are included. This is done because taking all sea states into account would lead to an unreasonable long computation time. However, sea states with a lower probability would have a minor effect on the selection, and the Shipmaster will avoid the heaviest wave conditions, thus the assumption is not critical. For the selections of the KVLCC2 propeller, a four bladed propeller is assumed and for the S175 propeller a five bladed because such propellers are commonly found on those types of vessels. The boundary conditions except for the cavitation criteria are defined as listed below:

$$\begin{aligned} &0.5 \leq P/D \leq 1.4\ (1.65) \\ &0.4\ (0.45) \leq A_e/A_0 \leq 1.00\ (1.05) \\ &0.3d \leq D \leq 2/3d \\ &76rpm \leq n \leq 110rpm \\ &0.6MCR \leq P_D \leq 0.9MCR \end{aligned} \tag{13}$$

The values between brackets are altered values for the S175. Moreover, the KVLCC2 nor the S175 have specific engine assigned, therefore it is assumed they use a slow running diesel engine without gearing system. The boundaries of the rotation speed are limited by average speed limits of such an engine found in [20] and power is limited by 60% and 90% of the maximum continuous rate (MCR) of the engine power, these percentages are commonly used. The MCR is estimated to be $P_E/0.5$.

Furthermore, both ships are simulated 5 times in several sea states for a period of 120 minutes in order to define the

simulation period to be used in the selection procedure. This period should ensure the accurate results and a reasonable computation time. The period is found by looking at the several moving averages in the sea states. For the KVLCC2 a 20 minute moving average is found to be sufficient (fig. 9) while for the S175 a 30 minutes moving average is required (fig. 10).

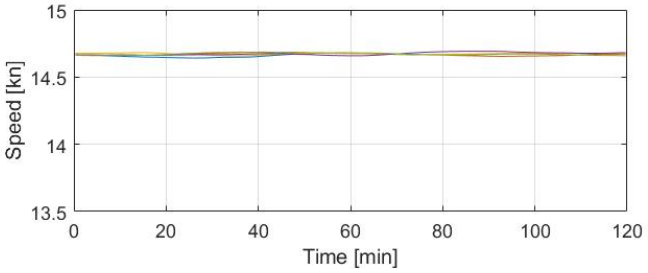

Fig. 9: 20 minute moving averages of the KVLCC2's speed in SS3

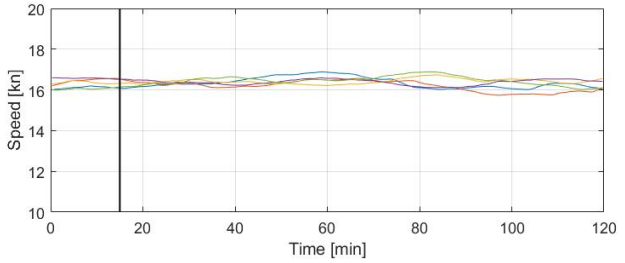

Fig. 10: 30 minute moving average of the S175's speed in SS3

A. Propeller selection for the KVLLC2

The results of these selection procedures for the KVLCC2 are summarised in table III. The characteristics of the propellers selected based on certain sea state are only minimally altered with respect to the propeller selected for still water. These minor changes only resulted in a negligible increase of delivered efficiency in the given sea state, additionally the selection in waves took a lot longer (6 seconds vs around 70 minutes).

As to explain the reason of such negligible differences, it must be considered that the propeller is deeply submerged ($14.4m$) and the KVLCC2 is a very large ship, thus its motions are not significantly amplified by the frequency ranges of the wave spectra found with higher probabilities. Furthermore, the propeller characteristics are not used in the inflow velocity model thus the changes are 'quasi' independent of the propeller. Another factor that could have contributed, is the underestimation of the added resistance for blunt hulls by the far-field method combined with the strip theory as this lowers the difference between still water and the sea states.

The selection procedure resulted only in a negligible increase in delivered efficiency in waves and took a lot longer than the selection procedure in still water. Therefore, it can be concluded that the operation of the propellers of such large ships is not significantly influenced by the presence of waves. So, the proposed selection procedure in waves is not practical for such type of ship.

	Still water	**SS1**	**SS2**	**SS3**
Acronym propeller	$KVL0P$	$KVL1P$	$KVL2P$	$KVL3P$
A_e/A_0	0.4788	0.4786	0.4792	0.4788
P/D	0.6447	0.6445	0.6451	0.6447
$D\ [m]$	10.246	10.247	10.244	10.246
$n\ [rpm]$	76	76	76	76
$\eta_{D,s,optimised}$		0.6309	0.6310011	0.6283390
$\eta_{D,s,KVLCC2.0P}$		0.6309	0.6310009	0.6283389
$\eta_{D,still}$	0.6309	0.6309	0.6309	0.6309
η_0	0.5155	0.5155	0.5155	0.5155
$\overline{U}_{optiwave}\ [kn]$	15.50	15.50	15.47	15.39
$\overline{U}_{optistill}\ [kn]$		15.50	15.47	15.39

TABLE III: Propellers selected for the KVLCC2 with still water resistance boundary conditions

B. Propeller selection for the S175

The propellers selected for the KVLCC2 in waves only had minor changes compared to the propeller selected in still water. It was posed that this might be caused by the size of the ship, therefore the same procedure is applied for a smaller containership, the S175. The main parameters of this ship are given in table IV.

$L_{PP}\ [m]$	175
$B\ [m]$	25.4
$d\ [m]$	9
$\Delta\ [ton]$	24252.55
C_B	0.57
$U_S\ [kn]$	19
$x_P\ [m]$	$-0.49L_{PP}$
$z_P\ [m]$	-6

TABLE IV: Ship particulars of the S175

As already previously mentioned the RAO of surge can not be calculated by that code. Hence, it is assumed to depend on λ/L_{PP} and weakly influenced of the ship shape. Thus, the non-dimensional curve used for the KVLCC2 is also assumed valid for the S175.

The results of the propeller selections are summarised in table V. The propeller selected based on SS1 did not result in any visible increase of efficiency because SS1 represents a relatively calm sea state. The delivered efficiency and ship's speed obtained in the scatter diagram selection, lay between the values of SS1 and SS2 because the average sea state of the reduced lays between those sea states.

Furthermore, a general trend over all the propellers is visible: the pitch ratio decreases when a propeller is selected for a more severe the sea-state while the required engine speed increases. The diameter did not change but stayed the maximal diameter defined by the boundary conditions, a lower diameter would require a higher engine speed to deliver sufficient thrust, yet a higher engine speed lowers the advance coefficient which tends to reduce the open water efficiency.

The reason for the changes is that due to the added resistance, the required thrust increases and therefore the ships speed

	Still water	SS1	SS2.0	SS3	Scatter
Acronym propeller	SWP	SS1.0P	SS2.0P	SS3.0P	SC.0P
A_e/A_0	0.643	0.642	0.638	0.626	0.649
P/D	1.117	1.115	1.107	1.082	1.098
$D\ [m]$	6	6	6	6	6
$n\ [rpm]$	99	99	99	101	100
$\eta_{D,s,optimised}$		0.7037	0.6974	0.6489	0.6988
$\eta_{D,s,SWP}$		0.7037	0.6971	0.6475	0.6986
$\eta_{D,still}$	0.7045	0.7045	0.7045	0.7041	0.7044
η_0	0.6643	0.6643	0.6643	0.6640	0.6642
$\overline{U}_{s,optimised}\ [kn]$	19	18.97	18.44	16.28	18.71
$\overline{U}_{s,SWP}\ [kn]$		18.97	18.44	16.27	18.71

TABLE V: Propellers selected for the S175 with still water resistance boundary conditions

decreases. This causes the average advance coefficient to lower and thus a shift to the left of the working point in the open water curves. In this new working point a lower pitch propeller has a better open water efficiency as the propeller is heavier loaded. This is illustrated in figure 11 for the selection in SS3.

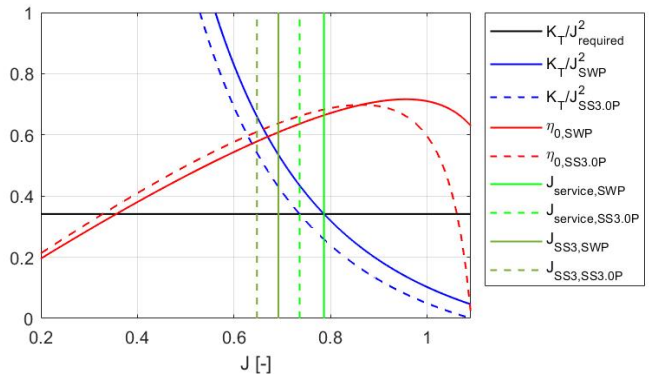

Fig. 11: Open water curves for SWP and SS3.0P and their average advance coefficients

The expanded blade area ratio does show a trend between the single sea state selections. The cause of this is that for a lower pitch ratio, the minimal expanded blade area ration given by Burill's cavitation criterion is lower. However, the effect of A_e/A_0 is negligible on the open water curves and the propeller selected for the scatter diagram does not follow this trend.

Although, these changes have a small positive effect on the delivered efficiency in the specific sea state, they have a similar but adverse effect on the efficiency in still water. Therefore, the effect can be considered to be negligible and it should be questioned if it will result in a noticeable effect on the fuel consumption and performance of the propeller.

Hence, the reasoning above was mainly based on the speed loss and propeller speed, it is questionable if the changes are due to the added resistance or if fluctuations due to waves had an influence. Furthermore the speed loss in SS1 and SS2 might be counteracted by the Shipmaster who increases the power to maintain the service speed.

In an attempt to see the effect of the fluctuations, a propeller is selected only taking in account the average added resistance in SS2 at service speed (ADP) and other propellers were selected by the proposed selection method but with the boundary conditions adapted for the higher required thrust in still water. Due to the fact that the increased resistance is already included, the upper limit of the power boundary condition is increased to 100% MCR. Furthermore, the engine speed in the simulations has been altered in such way that the propeller delivers the thrust required to propel the ship at service speed with the increased resistance. The selection procedure in waves has been executed twice for the same sea-state (SS2) but with a different wave profile (SS2.1 and SS2.2) in order to verify the repeatability of the procedure. The results are summarised in table VI.

	Added resistance	SS2.1	SS2.2	SS2.3
Acronym propeller	ADP	SS2.1P	SS2.2P	SS2.3P
A_e/A_0	0.6900	0.692	0.692	0.6902
P/D	1.063	1.067	1.068	1.064
$D\ [m]$	6	6	6	6
$n\ [rpm]$	106.2	105.9	105.8	106.1
$\eta_{D,s,optimised}$		0.6887	0.6888	0.6878
$\eta_{D,s,ADP}$		0.6887	0.6888	0.6878
$\eta_{D,still}$	0.6875	0.6875	0.6875	0.6875
η_0	0.6483	0.6483	0.6483	0.6483
$\overline{U}_{s,optimised}\ [kn]$	19	19.06	19.10	18.97
$\overline{U}_{s,ADP}\ [kn]$		19.06	19.10	18.97

TABLE VI: The propeller selected for still water taking into account the average added resistance in SS2 (ADP) and propellers selected for SS2 with boundary condition including the average added resistance (SS2.1P and SS2.2P)

The propeller selected based on the average resistance without taking into account the fluctuations and motions due to waves (ADP) has a higher expanded blade area, lower pitch and higher engine speed compared the original propeller selected in still water (SWP). This is explained by the fact that the required thrust is higher which is achieved by increasing the engine speed and thus the advance coefficient is lower. At the lower advance coefficient, a lower pitch ratio has a higher the open water efficiency. The expanded blade area is increased in order to satisfy the changed cavitation criterion, that now needs to be fulfilled for the thrust required to face the still water resistance plus the added resistance. This criterion is not satisfied for the SWP and the SS2.0P. Although these propellers do not satisfy this criterion, they are also simulated in SS2 with same wave profile for which SS2.1P was selected. In the simulation with SWP and SS2.0, the engine speed was

increased compared to the one given in table V, so that service speed could be maintained with the increase of average added resistance. The simulations resulted in a theoretical delivered efficiency in that sea state of 0.6865 and 0.6866 for SWP and SS2.0P respectively. These efficiencies are lower than achieved by ADP and SS2.2P. Moreover, this number is higher than in reality because cavitation will reduce the efficiency. How much the efficiency would be reduced cannot be estimated by the developed procedure and would require a more complete cavitation model to be included in the simulation code.

Furthermore, SS2.1P and SS2.2P are not exactly the same propeller. This is due to the different wave profile and the short simulation period. A longer simulation period might eliminate this inconsistency. However, both propellers have a higher pitch ratio, expanded blade area and lower engine speed.

These changes can be explained by the increase of the advance coefficient and thus explains why both SS2.1P and SS2.2P have a higher pitch ratio. The higher pitch ratio implies that the engine speed has to slightly decrease to balance the higher thrust delivered by these propellers. The open water curves of SS2.1P and are compared to ADP in figure 12 where the increase of the advance coefficient is illustrated. This is increase is caused by a raise of the mean advance speed which has two roots: raise due to pitching of the ship (eq. 8) and the higher ships speed. The higher ships speed appears to contradict the lower thrust coefficient for the working point with the higher advance coefficient. However, due to the 'quasi' regular wave approach used for calculation of the added resistance, the average total resistance in the simulation was around 2% lower than the estimated one used to define the propeller speed. In addition to the elevated pitch ratio, the expanded blade area ratio increased in order to satisfy the cavitation boundary condition.

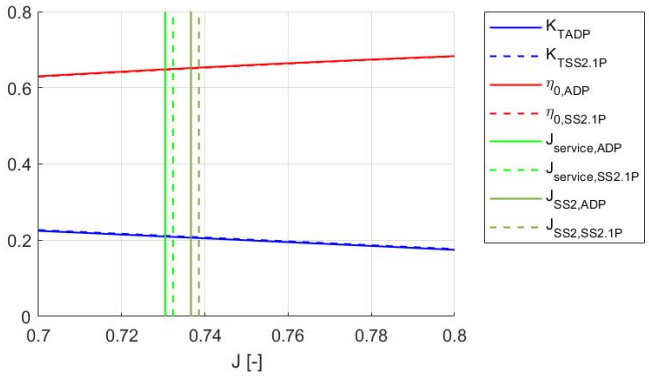

Fig. 12: Open water curves for ADP and SS2.1P and their average advance coefficients

In order to have a better view on the effect of the waves, the same propeller selection is repeated but the average added resistance in the simulation is calculated by the wave spectrum instead of the 'quasi' regular wave approach. The propeller selected with this procedure (SS2.3P in table VI) had a slightly higher pitch ratio than ADP , slightly higher expanded blade area ration and a lower engine speed . Just as earlier, the lower engine speed is a consequence of the higher pitch ratio. However, in this simulation the average ship's speed was lower than the service speed. This is explained by the increase of average advance speed due to pitching of the ship (eq. 8) that causes a the advance coefficient to increase as shown in figure 13. Just as it was the case for the selections with the 'quasi' regular wave approach, this increase of advance coefficient causes a propeller with higher pitch ratio to be more efficient. However, unlike in those simulations, here the lower thrust is not compensated by the lower added resistance and thus the ship slowed down.

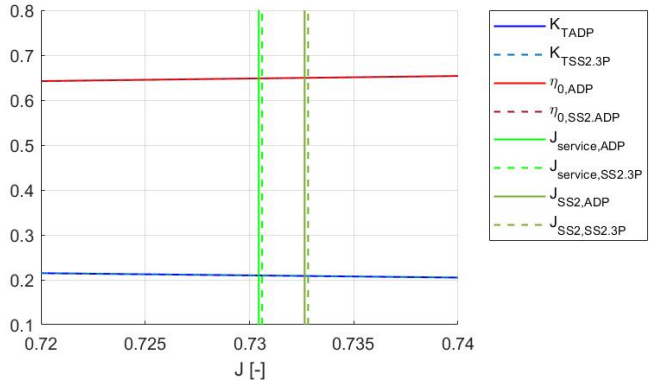

Fig. 13: Open water curves for ADP and SS2.3P and their average advance coefficients

Regardless of this trend, the differences between the propellers including the effect of waves and the ADP propeller are minimal and the increase of delivered efficiency in waves negligible. Thus, it can be concluded that the differences are small and will not have a significant effect on the fuel consumption, however it is recommended to select a propeller taking the added resistance in mind because this will reduce the cavitation when the resistance increases in presence of waves. Moreover, it will improve the real life efficiency.

V. Conclusion

In this work, a selection procedure of the Wageningen B-series propeller based on real weather conditions was proposed and compared to the optimal propeller selected in still water.

The best propeller for the KVLCC2 in several sea states was selected. The differences between the propeller selected in a given sea state and the one selected in still water were negligible. This was explained by the fact that the propeller is deeply submerged and the ship is large, so waves have no significant effect. Therefore, the propeller selection procedure is not found useful for large and slow ships.

In order to see if the proposed propeller selection procedure would be useful for smaller ships, it was applied to the S175. Some tendencies have been noticed on the propeller selected for sea state of increased severity. In particular a lower pitch ratio and a higher engine speed. These changes were more pronounced for more severe sea states. The reason

for these changes was due to the added resistance, the required thrust increased and therefore the speed decreased. In this selection procedure, as well as for the KVLCC2, the propeller speed was set equal to the propeller speed required to sail at service speed in still water, therefore it was proposed that it might be more realistic to change the propeller speed to the one required to sail the ship at service speed in still water including the average resistance for a given sea state. This modified procedure resulted in small changes of the propeller which could be explained by the increase of the advance coefficient and the cavitation criterion of Burill [19]. However, the differences between those propellers including the fluctuations due to waves and the one selected in still water including the average resistance for a given sea state were small and the increase of efficiency negligible. Therefore, it is concluded that the proposed selection procedure is not worth considering in the selection of a propeller. It is best to select a propeller just taking into account the average added resistance to lower the risk cavitation and improve the real life efficiency. This average resistance depends on where the ship is expected to sail for example if the ship is expected to sail mostly in the North Atlantic, the added resistance can be taken to represent the ship operating in the average sea state of the DNV North Atlantic scatter diagram. Furthermore both ships (KVLCC2 and S175) are still big ships and ventilation was not present in SS1 and SS2. Repeating the selection procedure for an even smaller ship such as a fishing vessel might result in bigger improvements.

It was further noted that the inclusion of a more comprehensive cavitation model embedded in the simulation code itself, might influence the results in such a way that the differences with the still water optimal propeller are greater. However, it should first be verified for a single simulation whether such a model has a noticeable effect on performance.

Furthermore, the propeller was given a constant rotational speed which is not a realistic model. This model was chosen because the averages with and without an engine model are comparable [3]. However, this affects the torque fluctuations and implementing a more complex engine model would be more accurate and lead to a better analysis. Furthermore, a better engine model would allow to compare fuel consumption rather than efficiency.

On a final note it must be said that all the propellers were selected for the ship in loaded condition while this does not reflects the reality. Therefore, it can be interesting to adapt the code as such that it includes ballast and loaded condition. I could be expected that this will change the results because the propeller will be more prone to cavitation and ventilation in ballast condition. However, the trends noticed for the S175 will remain because they are mostly based on reasoning of the advance coefficient.

REFERENCES

[1] O. Faltinsen, K. Minsaas, N. Liapis, and S. Skjordal, "Prediction of resistance and propulsion of a ship in a seaway," *Thirteenth Symposium on Naval Hydrodynamics*, pp. 505–529, 1980.

[2] IMO, "Greenhouse Gas Emissions." http://www.imo.org/en/OurWork/Environment/PollutionPrevention/AirPollution/Pages/GHG-Emissions.aspx, 2020. Accessed on: May 8, 2020.

[3] B. Taskar, K. K. Yum, S. Steen, and E. Pedersen, "The effect of waves on engine-propeller dynamics and propulsion performance of ships," *Ocean Engineering*, vol. 122, pp. 262–277, 2016.

[4] N. Vitali, J. Prpić-Oršić, and C. Guades Soares, "Uncertainties related to the estimation of added resistance of a ship in waves," in *Maritime Technology and Engineering III*, vol. 1, pp. 391–399, CRC Press, jun 2016.

[5] N. Vitali, J. Prpić-Oršić, and C. Guedes Soares, "Methods for Added Resistance Estimation in Head and Oblique Seas," *Book of Abstract of the 22nd Symposium on Theory and Practice of Shipbuilding, In Memoriam prof. Leopold Sorta*, p. 17, 2016.

[6] J. Holtrop and G. Mennen, "An approximate power prediction method," *Internation Shipbuilding progress*, vol. 29, no. 335, pp. 166–170, 1982.

[7] N. Salvesen, E. Tuck, and O. Faltinsen, "Ship Motions and Sea Loads," *Transactions of the Society of Naval Architects and Marine Engineers*, vol. 78, pp. 250–287, 1970.

[8] N. Salvesen, "Added Resistance of Ships in Waves," *Journal of Hydronautics*, vol. 12, pp. 24–34, jan 1978.

[9] M. Ueno, Y. Tsukada, and K. Tanizawa, "Estimation and prediction of effective inflow velocity to propeller in waves," *Journal of Marine Science and Technology (Japan)*, vol. 18, pp. 339–348, sep 2013.

[10] J. Prpić-Oršić and O. M. Faltinsen, "Estimation of ship speed loss and associated CO^2 emissions in a seaway," *Ocean Engineering*, vol. 44, pp. 1–10, 2012.

[11] K. Minsaas, O. Faltinsen, and B. Persson, "On the importance of added resistance, propeller immersion and propeller ventilation for large ships in a seaway," *Proceedings of the 2nd international symposium on practical design in shipbuilding. Tokyo & Seoul, Japan*, 1983.

[12] O. N. Smogeli, *Control of marine propellers: from normal to extreme conditions*. PhD thesis, NTNU, 2006.

[13] J. Holtrop and G. Mennen, "A statistical power prediction method," *Internation Shipbuilding progress*, vol. 24, no. 270, pp. 253–256, 1978.

[14] H. Sadat-Hosseini, P.-c. Wu, P. M. Carrica, H. Kim, Y. Toda, and F. Stern, "CFD verification and validation of added resistance and motions of KVLCC2 with fixed and free surge in short and long head waves," *Ocean Engineering*, vol. 59, pp. 240–273, feb 2013.

[15] M. W. Oosterveld and P. van Oossanen, "Further Computer-Analyzed Dat of the Wageningen B-Screw Series.," *International Shipbuilding Progress*, vol. 22, no. 251, pp. 251–262, 1975.

[16] D. Moor and D. Murdey, "Motions and propulsion of single screw models in head seas-2," *Roy Inst Nav Architects Quart Trans*, vol. 112, no. 2, pp. 121–164, 1970.

[17] B. Taskar, *The Effect of Waves on Marine Propellers and Propulsion*. Phd thesis, NTNU, may 2017.

[18] H. Søding, "Program PDSTRIP: Public Domain Strip Method (manual)," 2006.

[19] L. Burrill and A. Emerson, "Propeller cavitation: Further tests on 16in. propeller models in the King's College cavitation tunnel1," *International Shipbuilding Progress*, vol. 10, pp. 119–131, apr 1963.

[20] MAN Diesel, "MAN B & W 70-60 ME-GI / -C-GI-TII Type Engines Engine Selection Guide Electronically Controlled Two stroke Engines," *MAN Diesel*, vol. 1, jun 2010.